

Exciton drag and drift induced by a two-dimensional electron gas

S. K. Lyo

*Sandia National Laboratories, Albuquerque, New Mexico 87185, USA**
and Korea Advanced Institute of Science and Technology (KAIST), Taejeon, S. Korea

(Received 14 October 2004; revised manuscript received 7 December 2004; published 22 March 2005)

We show theoretically that an electric current in a high-mobility quasi-two-dimensional electron layer induces a significant drift of excitons in an adjacent layer through interlayer Coulomb interaction. The exciton gas is shown to drift with a velocity which can be a significant fraction of the electron drift velocity at low temperatures. The estimated drift length is of the order of micrometers or larger during the typical exciton lifetime for GaAs/Al_xGa_{1-x}As double quantum wells. A possible enhancement of the exciton radiative lifetime due to the drift is discussed.

DOI: 10.1103/PhysRevB.71.115317

PACS number(s): 71.35.-y, 73.63.Hs, 78.67.De

I. INTRODUCTION

Excitons are good storage source of light energy and play an increasingly important role in recent optoelectronic applications. The motion of excitons in solids has been studied for a long time.¹⁻³ Excitons cannot be accelerated by an external field due to their charge neutrality in contrast to charged particles. Recently, it was demonstrated that Wannier-Mott excitons can be transported at the speed of sound in polar semiconductor quantum wells (QWs) using surface acoustic waves.^{4,5} In this paper, we propose a new mechanism which can cause Wannier-Mott excitons to drift even at a faster speed over a large distance during its radiative lifetime in semiconductor quantum wells at low temperatures. We also discuss the possibility that the exciton drift can enhance the exciton lifetime significantly.

We consider an *n*-doped asymmetric double-QW structure such as GaAs/Al_xGa_{1-x}As illustrated in Fig. 1. The left QW (QW1) carries an electron gas, while the right QW (QW2) has photo-generated low-density excitons. The electron gas is not affected by the low-power generation of electron-hole pairs. Carrier tunneling across the center barrier is assumed to be negligible. The electron gas has a very high mobility μ and drifts fast under an external field \mathbf{E} applied in QW1. The electrons interact across the barrier with the excitons through a monopole-dipole interaction and impart their drift momentum to the excitons, causing them to drift in the same direction. This phenomenon is similar to the well-known Coulomb-drag effect where an electric current in one QW induces a voltage in the second electron gas in the adjacent QW.^{6,7}

We calculate the ratio of the drift velocities in the exciton gas and the electron gas. We find that a high-mobility electron gas induces a significant drift of excitons with a velocity which can be a significant fraction of the electron drift velocity. The drift ratio is restricted by the resistive force against the exciton motion, which is represented by the transport relaxation time. The contribution to the latter from scattering by phonons and interface roughness is calculated. The estimated drift length is on the order of micrometers during the typical exciton lifetime of \sim a nanosecond for GaAs/Al_xGa_{1-x}As double-quantum wells.

II. FORMALISM

The electron gas in QW1 transfers momentum \mathbf{P} to the excitons in QW2 at a rate⁷

$$\frac{d\mathbf{P}}{dt} = \frac{2\pi}{\hbar} \sum_{\mathbf{k}, \mathbf{K}, \mathbf{q}} |V(\mathbf{q}_{\parallel})|^2 \hbar \mathbf{q}_{\parallel} [f_{\mathbf{k}}(1 - f_{\mathbf{k}-\mathbf{q}_{\parallel}})g_{\mathbf{K}} - f_{\mathbf{k}-\mathbf{q}_{\parallel}}(1 - f_{\mathbf{k}})g_{\mathbf{K}+\mathbf{q}_{\parallel}}] \delta(\varepsilon_{\mathbf{k}} + E_{\mathbf{K}} - \varepsilon_{\mathbf{k}-\mathbf{q}_{\parallel}} - E_{\mathbf{K}+\mathbf{q}_{\parallel}}), \quad (1)$$

which is the interlayer two-particle scattering rate times the momentum transfer $\hbar \mathbf{q}_{\parallel}$. In Eq. (1), $V(\mathbf{q}_{\parallel})$ is the Coulomb interaction between the electrons in QW1 and the excitons in QW2, $\varepsilon_{\mathbf{k}} = (\hbar k)^2/2m^*$ is the electron energy, and $E_{\mathbf{K}} = (\hbar K)^2/2M$ is the exciton kinetic energy. Here m^* is the effective electron mass in QW1 and can be different from the effective electron mass m_e of the exciton in QW2. The quantity $M = m_e + m_h$ is the total mass of the exciton, where m_h is the effective hole mass. The quantities \mathbf{k} and \mathbf{K} are the two-dimensional wave vectors for the electron motion and the center-of-mass motion of the exciton, respectively. The validity of the Born approximation in Eq. (1) for the relevant parameters in the present problem will be discussed later. When an external dc field \mathbf{E} is applied in QW1, the electron and exciton distribution functions are given to the first order in E by⁸

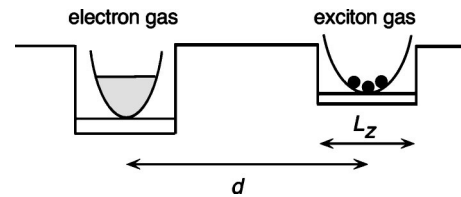


FIG. 1. (a) A schematic diagram of a double-quantum-well structure with an electron gas in the left QW (QW1) and an exciton gas in the right QW (QW2). The two QWs are separated at a distance d and L_z is the width of QW2.

$$f_{\mathbf{k}} = f_{\mathbf{k}}^{(0)} - \frac{\partial f_{\mathbf{k}}^{(0)}}{\partial \mathbf{k}} \cdot \Delta \mathbf{k}_e, \quad g_{\mathbf{K}} = g_{\mathbf{K}}^{(0)} - \frac{\partial g_{\mathbf{K}}^{(0)}}{\partial \mathbf{K}} \cdot \Delta \mathbf{K}_{ex}, \quad (2)$$

where $f_{\mathbf{k}}^{(0)}, g_{\mathbf{K}}^{(0)}$ are the equilibrium Fermi function and the Boltzmann distribution for the electrons and excitons, respectively. Here, we assume that the excitons are incoherent and in equilibrium with the same lattice temperature as the electrons in the absence of the field. The validity and the limitations of the present model will be discussed later. The quantities $\Delta \mathbf{k}_e = e\tau_e \mathbf{E}/\hbar$ and $\Delta \mathbf{K}_{ex} \propto \mathbf{E}$ are the field-induced displacements for the electron and the exciton gas. Here, τ_e is the relaxation time of the electron gas at low temperatures (T). The exciton drift $\Delta \mathbf{K}_{ex}$ is induced through electron-exciton collision and is to be determined self-consistently.

The Coulomb interaction between an electron in QW1 and the electron inside an exciton in QW2 is given by

$$V_{ee}(\mathbf{q}_{\parallel}) = \frac{e^2}{\kappa \epsilon(q_{\parallel}) S^2} \int \int \int \frac{e^{i(\mathbf{k}-\mathbf{k}') \cdot \mathbf{r}_{1,\parallel}} e^{i(\mathbf{K}-\mathbf{K}') \cdot \mathbf{R}_{2,\parallel}}}{|\mathbf{r}_1 - \mathbf{r}_{2e,\parallel}|} \times |\phi_1(z_1) \psi(\mathbf{r}_{2,\parallel}, z_{2e}, z_{2h})|^2 d^3 r_1 d^3 r_{2e} d^3 r_{2h}, \quad (3)$$

where \mathbf{k} (\mathbf{k}') and \mathbf{K} (\mathbf{K}') are the initial (final) in-plane wave vectors of the electron and the exciton, respectively, $\mathbf{q}_{\parallel} = \mathbf{k}' - \mathbf{k}$, κ is the average bulk dielectric constant, and S is the cross sectional area of the QWs. In Eq. (3), $\phi_1(z_1)$ is the confinement wave function in QW1 and $\psi(\mathbf{r}_{2,\parallel}, z_{2e}, z_{2h})$ is the exciton wave function for the $1s$ ground state. The random phase approximation (RPA) is employed for the dielectric function $\epsilon(q_{\parallel})$ of the electron gas. The center-of-mass and relative in-plane coordinates of the exciton are given by

$$\mathbf{R}_{2,\parallel} = \alpha_e \mathbf{r}_{2e,\parallel} + \alpha_h \mathbf{r}_{2h,\parallel}, \quad \mathbf{r}_{2,\parallel} = \mathbf{r}_{2e,\parallel} - \mathbf{r}_{2h,\parallel}, \quad (4)$$

where $\alpha_e = m_e/M$, $\alpha_h = m_h/M$, and z_{2e}, z_{2h} indicate the z coordinates of the electron and the hole of the exciton in the direction perpendicular to the QW.

A variational wave function is employed for the exciton wave function $\psi(\mathbf{r}_{2,\parallel}, z_{2e}, z_{2h})$. This function is given, for the purpose of estimating the order-of-magnitude of the drag effect, by

$$\psi(\mathbf{r}_{2,\parallel}, z_{2e}, z_{2h}) = \varphi(\mathbf{r}_{2,\parallel}) \phi_{2e}(z_{2e}) \phi_{2h}(z_{2h}), \quad (5)$$

where $\varphi(\mathbf{r}_{2,\parallel}) = (2\sqrt{2}\lambda/a_B\sqrt{\pi}) \exp(-2\lambda r_{2,\parallel}/a_B)$, a_B is the bulk exciton radius in GaAs, and λ is the variational parameter. A more general expression $\varphi(\mathbf{r}_{2,\parallel}) \propto \exp(-[a_{\parallel}^2 r_{2,\parallel}^2 + a_z^2 (z_{2e} - z_{2h})^2]^{1/2})$ with two variational parameters a_{\parallel}, a_z was employed in an earlier investigation⁹ of the exciton binding energy in a QW. According to this result, the two-dimensional (2D) form of the variational function in Eq. (5) (i.e., with $a_z=0$) yields an excellent ground-state binding energy when the width L_z of QW2 is not too large, e.g., $L_z \lesssim 4a_B$ for an infinitely deep well.⁹ In this range, λ decreases from the 2D limit $\lambda=1$ at $L_z=0$ to about $\lambda \sim 0.4$ near $L_z=4a_B$. Equation (3) is then simplified as

$$V_{ee}(\mathbf{q}_{\parallel}) = \frac{2\pi e^2 \varphi_{e,\mathbf{q}_{\parallel}}}{q_{\parallel} \kappa \epsilon(q_{\parallel}) S} \delta_{\mathbf{k}+\mathbf{K}, \mathbf{k}'+\mathbf{K}'} \int \int |\phi_1(z_1) \phi_{2e}(z_{2e})|^2 \times e^{-q_{\parallel} |d+z_{2e}-z_1|} dz_1 dz_{2e}, \quad (6)$$

where

$$\varphi_{e,\mathbf{q}_{\parallel}} = \int \exp(i\mathbf{q}_{\parallel} \cdot \alpha_h \mathbf{r}_{2,\parallel}) |\varphi(\mathbf{r}_{2,\parallel})|^2 d^2 r_{2,\parallel} = [(q_{\parallel} \alpha_h a_B / 4\lambda)^2 + 1]^{-3/2}, \quad (7)$$

and d is the center-to-center distance between the two QWs. A similar expression is obtained for electron-hole interaction $V_{eh}(\mathbf{q}_{\parallel})$ with an opposite sign.

The integrations in Eq. (6) can be carried out numerically. However, for simplicity, we ignore the fluctuation around the average distance d , obtaining $e^{-q_{\parallel} d}$ for the integral. This approximation ignores the fact that the electron in QW1 and the electron and the hole of the exciton can be closer or farther away than the average distance d in the z direction due to the spread of the wave function in the QWs. This approximation underestimates $V_{ee}(\mathbf{q}_{\parallel})$ somewhat and thus the drag effect because stronger interaction at a closer distance (i.e., $z_{2e}-z_1 < 0$) turns out to overcompensate the weaker interaction at a larger distance (i.e., $z_{2e}-z_1 > 0$) slightly.³ It is to be noted at this point that our numerical result becomes independent of the width of QW1 with this approximation. Adding the two contributions from $V_{ee}(\mathbf{q}_{\parallel})$ and $V_{eh}(\mathbf{q}_{\parallel})$ and defining $V_{ee}(\mathbf{q}_{\parallel}) + V_{eh}(\mathbf{q}_{\parallel}) \equiv V(\mathbf{q}_{\parallel}) \delta_{\mathbf{k}+\mathbf{K}, \mathbf{k}'+\mathbf{K}'}$, we find

$$V(\mathbf{q}_{\parallel}) = \frac{2\pi e^2}{q_{\parallel} \kappa \epsilon(q_{\parallel}) S} e^{-q_{\parallel} d} (\varphi_{e,\mathbf{q}_{\parallel}} - \varphi_{h,\mathbf{q}_{\parallel}}), \quad (8)$$

where $\varphi_{h,\mathbf{q}}$ is obtained from Eq. (7) by replacing $\alpha_h \rightarrow \alpha_e$.

Inserting Eq. (2) in Eq. (1) and using a detailed balance, we find, after a lengthy algebra,

$$\frac{d\mathbf{P}}{dt} = \frac{\hbar}{\tau_{12}} \left(\Delta \mathbf{k}_e - \frac{m^*}{M} \Delta \mathbf{K}_{ex} \right), \quad (9)$$

where

$$\frac{1}{\tau_{12}} = \frac{\pi \hbar}{k_B T m^*} \sum_{\mathbf{k}, \mathbf{K}, \mathbf{q}_{\parallel}} |q_{\parallel} V(\mathbf{q}_{\parallel})|^2 f_{\mathbf{k}}^{(0)} (1 - f_{\mathbf{k}-\mathbf{q}_{\parallel}}^{(0)}) g_{\mathbf{K}}^{(0)} \delta(\epsilon_{\mathbf{k}} + E_{\mathbf{K}} - \epsilon_{\mathbf{k}-\mathbf{q}_{\parallel}} - E_{\mathbf{K}+\mathbf{q}_{\parallel}}). \quad (10)$$

In a steady state, the drag force in Eq. (9) is balanced by the resistive force due to scattering inside QW2, yielding

$$\frac{d\mathbf{P}}{dt} = n_{ex} \hbar \frac{\Delta \mathbf{K}_{ex}}{\tau_{ex}}, \quad (11)$$

where τ_{ex}^{-1} is the thermally averaged transport relaxation time⁸ of the excitons to be calculated later. We set the total number of the excitons $n_{ex} \equiv 1$ to unity for convenience without loss of generality. Equations (9) and (11) then yield

$$\Delta \mathbf{V}_{ex} = \mathcal{R} \Delta \mathbf{v}_e; \mathcal{R} = \frac{m^*/M \tau_{12}}{1/\tau_{ex} + m^*/M \tau_{12}}, \quad (12)$$

where $\Delta \mathbf{V}_{ex} = \hbar \Delta \mathbf{K}_{ex}/M$, $\Delta \mathbf{v}_e = \hbar \Delta \mathbf{k}_e/m^*$ are the exciton and electron drift velocities, respectively, and $g_{\mathbf{K}}^{(0)}$

$=\exp(-E_{\mathbf{K}}/k_B T)/Z$ with $Z=\sum_{\mathbf{K}}\exp(-E_{\mathbf{K}}/k_B T)$. In the limit of zero resistance for the exciton motion i.e., $1/\tau_{ex}=0$, Eq. (12) yields $\Delta\mathbf{V}_{ex}=\Delta\mathbf{v}_e$. Namely, the excitons drift with the same drift velocity of the electrons as expected. The drift velocity of the excitons is smaller than that of the electrons otherwise (i.e., $\mathcal{R}<1$).

III. EXCITON SCATTERING RATE

In this section, we calculate the exciton momentum relaxation rate $1/\tau_{ex}$ introduced in Eq. (11) as a function of T by considering exciton-phonon and exciton-surface-roughness scattering. The Boltzmann equation can be constructed for the exciton gas using the analogy with the electron transport. Defining $\mathbf{P}=\hbar\mathbf{K}$, Eq. (9) can be rewritten in the form $\hbar d\mathbf{K}/dt=\mathbf{F}$, where the driving force \mathbf{F} is given by the quantity on the right hand side of Eq. (9). This force plays the role of the force $e\mathbf{E}$ from an external electric field for the transport of an electron gas. The derivation of the Boltzmann equation for the exciton gas driven by \mathbf{F} is analogous to that of the electron gas driven by $\mathbf{F}=e\mathbf{E}$ and is straightforward.^{8,10} In order to use the well-known results of Ziman⁸ and Holstein,¹⁰ we define $\Phi_{\mathbf{K}}\equiv\mathbf{V}_{\mathbf{K}}\cdot\hbar\Delta\mathbf{K}_{ex}$ in the second term of $g_{\mathbf{K}}$ in Eq. (2), where $\mathbf{V}_{\mathbf{K}}=\partial E_{\mathbf{K}}/\partial\hbar\mathbf{K}$, and obtain

$$\mathbf{V}_{\mathbf{K}}\cdot\mathbf{F}+\sum_{\mathbf{K}'}W_{\mathbf{K},\mathbf{K}'}(\Phi_{\mathbf{K}'}-\Phi_{\mathbf{K}})=0. \quad (13)$$

Here, $W_{\mathbf{K},\mathbf{K}'}=W_{\mathbf{K},\mathbf{K}'}^{ex-p}+W_{\mathbf{K},\mathbf{K}'}^{ex-sr}$ is the scattering rate due to exciton-phonon ($ex-p$) and exciton-surface-roughness ($ex-sr$) scattering between states \mathbf{K} and \mathbf{K}' and will be studied in the following. Holstein's result¹⁰ corresponds to $\mathbf{F}=\mathbf{u}$ in Eq. (13), where \mathbf{u} is the unit vector in the field direction. The standard relaxation-time (τ_{tr}) approximation corresponds to setting $\Phi_{\mathbf{K}}=\mathbf{V}_{\mathbf{K}}\cdot\mathbf{F}\tau_{tr}$ in Eq. (13), namely $\mathbf{F}=\hbar\Delta\mathbf{K}_{ex}\tau_{tr}^{-1}$, thereby identifying $\tau_{ex}=\tau_{tr}$ in Eq. (11) as the transport relaxation time.

A. Exciton-phonon scattering

It is sufficient to consider scattering by acoustic phonons at low temperatures. We first look for a solution of the form $\Phi_{\mathbf{K}}=\mathbf{V}_{\mathbf{K}}\cdot\mathbf{F}\tau_{ex-p}$ by ignoring the scattering-in term ($\propto\Phi_{\mathbf{K}'}$) in Eq. (13). This approximation yields an exact result for isotropic scattering, where $W_{\mathbf{K},\mathbf{K}'}$ is independent of the angle between \mathbf{K} and \mathbf{K}' . A correction to this approximation will be discussed later. The thermal average of the scattering rate is then given by

$$\begin{aligned} \frac{1}{\tau_{ex-p}} &= \frac{1}{Z} \sum_{\mathbf{K},\mathbf{K}'} \exp(-E_{\mathbf{K}}/k_B T) W_{\mathbf{K},\mathbf{K}'}^{ex-p} \eta_{\mathbf{K},\mathbf{K}'} \\ W_{\mathbf{K},\mathbf{K}'}^{ex-p} &= \frac{2\pi}{\hbar} \sum_{\mathbf{q}} \sum_{\pm} |V_{e-p}(\mathbf{q})|^2 P(q_z) \left(n_{\mathbf{q}} + \frac{1}{2} \pm \frac{1}{2} \right) \\ &\quad \times \delta(E_{\mathbf{K}} \pm \hbar\omega_{\mathbf{q}} - E_{\mathbf{K}}) \delta_{\mathbf{K}',\mathbf{K}+\mathbf{q}}, \end{aligned} \quad (14)$$

where $\eta_{\mathbf{K},\mathbf{K}'}=1$ in the present approximation and the sum-

mation on the wave vector $\mathbf{q}=(\mathbf{q}_{\parallel},q_z)$ includes the summation over the longitudinal ($s=l$) and transverse ($s=t$) phonon modes s . In Eq. (14), the upper (lower) sign corresponds to one-phonon emission (absorption), $\hbar\omega_{\mathbf{q}}$ is the phonon energy, and $n_{\mathbf{q}}$ is the Bose function. The barrier of the QW is assumed to be infinitely high, yielding $\phi_{2e}(z)=\phi_{2h}(z)$ in Eq. (5). The form factor $P(q_z)$ is then given by

$$P(q_z) = \left| \int e^{iq_z z} |\phi_{2e}(z)|^2 dz \right|^2 = \left(\frac{\pi^2 \sin(q_z L_z/2)}{(q_z L_z/2)[\pi^2 - (q_z L_z/2)^2]} \right)^2, \quad (15)$$

where L_z is the width of QW2. The square of the strength of the exciton-phonon interaction is given by^{2,11}

$$\begin{aligned} |V_{e-p}(\mathbf{q})|^2 &= \frac{\hbar\omega_{\mathbf{q}}}{2\epsilon(\mathbf{q}_{\parallel})^2 \rho c_s^2 \Omega} \left[(D_c \varphi_{e,\mathbf{q}_{\parallel}} - D_v \varphi_{h,\mathbf{q}_{\parallel}})^2 \delta_{s,l} \right. \\ &\quad \left. + (eh_{14})^2 \frac{A_s}{q^2} (\varphi_{e,\mathbf{q}_{\parallel}} - \varphi_{h,\mathbf{q}_{\parallel}})^2 \right], \end{aligned} \quad (16)$$

where ρ is the mass density, c_s the sound velocity, Ω the sample volume, D_c (D_v) the deformation potential for the conduction (valence) band indicated by the subscript c (v), h_{14} the piezoelectric coefficient, and

$$A_l = \frac{9q_{\parallel}^4 q_z^2}{2q^6}, \quad A_t = \frac{8q_{\parallel}^2 q_z^4 + q_{\parallel}^6}{4q^6}. \quad (17)$$

B. Exciton scattering by surface roughness

Surface roughness causes fluctuation of the potential energy $V_{sr}(\mathbf{r}_e, \mathbf{r}_h)$ when the position of the electron \mathbf{r}_e or the hole \mathbf{r}_h is near the interface. For the present analysis, we assume that the layer fluctuation is only at one of the interface at $z_{e,h}=L_z/2$ as usually is the case for GaAs/Al_xGa_{1-x}As QWs. The contributions to the roughness potential from the conduction and valence bands are given by¹²

$$\begin{aligned} V_c(\mathbf{r}_e) &= V_c^{(o)} \delta L(\mathbf{r}_{e,\parallel}) \delta(z_e - L_z/2), \\ V_v(\mathbf{r}_h) &= V_v^{(o)} \delta L(\mathbf{r}_{h,\parallel}) \delta(z_h - L_z/2), \end{aligned} \quad (18)$$

where $V_c^{(o)} \equiv V_e^{(o)} > 0$ ($V_v^{(o)} \equiv -V_h^{(o)} < 0$) is the algebraic conduction (valence) band offset and $\delta L(\mathbf{r}_{e,h,\parallel})$ is the layer-fluctuation amplitude. In the hole representation, $V_h^{(o)}$ is positive for type-I QWs. For infinitely large barrier height, the scattering matrix of Eq. (18) includes the following factors:¹²

$$\lim_{V_{\alpha}^{(o)} \rightarrow \infty} V_{\alpha}^{(o)} |\phi_{2\alpha}(z_{2\alpha})|^2 = \frac{\hbar^2}{m_{\alpha} L_z^3} \quad (\alpha = e, h), \quad (19)$$

which, when multiplied by the prefactor $\delta L(\mathbf{r}_{\alpha,\parallel})$ in Eq. (18), yields naturally the energy fluctuation $\delta\epsilon_{\alpha}(\mathbf{r}_{\alpha,\parallel}) = \hbar^2 \delta L(\mathbf{r}_{\alpha,\parallel}) / m_{\alpha} L_z^3$ for the ground sublevel of a particle in a box of length L_z at $\mathbf{r}_{\alpha,\parallel}$.

The matrix element for the exciton-roughness potential $V_{sr}(\mathbf{r}_e, \mathbf{r}_h) = V_c(\mathbf{r}_e) + V_v(\mathbf{r}_h)$ is obtained extending the result for deformation scattering in Eq. (16) and is given by²

$$\langle \mathbf{K}' | V_{sr} | \mathbf{K} \rangle = \frac{1}{2\pi S} \int dq_z (G(\alpha_h \mathbf{q}_{\parallel}, q_z) V_c(\mathbf{q}_{\parallel}, q_z) - G(-\alpha_e \mathbf{q}_{\parallel}, q_z) V_v(\mathbf{q}_{\parallel}, q_z)), \quad (20)$$

where $\mathbf{q}_{\parallel} = \mathbf{K}' - \mathbf{K}$,

$$V_{\alpha}(\mathbf{q}_{\parallel}, q_z) = \int V_{\alpha}(\mathbf{r}) e^{-i\mathbf{q}_{\parallel} \cdot \mathbf{r}} d^3 r \quad (\alpha = c, v) \quad (21)$$

and

$$G(\mathbf{q}_{\parallel}, q_z) = \int \int \int |\psi(\mathbf{r}_{\parallel}, z_e, z_h)|^2 \exp(i\mathbf{q}_{\parallel} \cdot \mathbf{r}_{\parallel} + iq_z z_e) d^2 r_{\parallel} dz_e dz_h. \quad (22)$$

Introducing a Gaussian approximation for the ensemble average,

$$\langle \delta L(\mathbf{r}'_{\parallel}) \delta L(\mathbf{r}_{\parallel}) \rangle_{av.} = \delta b^2 \exp(-(\mathbf{r}'_{\parallel} - \mathbf{r}_{\parallel})^2 / \Lambda^2), \quad (23)$$

where δb is the fluctuation amplitude, Λ the correlation length, and using Eqs. (18)–(23), we find

$$\langle |\langle \mathbf{K}' | V_{sr} | \mathbf{K} \rangle|^2 \rangle_{av.} = \frac{\pi}{S} \left(\frac{\Lambda \delta b}{L_z} \right)^2 \exp(-q_{\parallel}^2 \Lambda^2 / 4) \left(\frac{\varphi_{e, \mathbf{q}_{\parallel}} \hbar^2}{m_e L_z^2} + \frac{\varphi_{h, \mathbf{q}_{\parallel}} \hbar^2}{m_h L_z^2} \right). \quad (24)$$

The relaxation-time expression $\Phi_{\mathbf{K}} = \mathbf{V}_{\mathbf{K}} \cdot \mathbf{F} \tau_{ex-sr}$ introduced earlier yields an exact solution to Eq. (13) in this case with

$$\frac{1}{\tau_{ex-sr}} = \frac{1}{Z} \sum_{\mathbf{K}, \mathbf{K}'} \exp(-E_{\mathbf{K}} / k_B T) W_{\mathbf{K}, \mathbf{K}'}^{ex-sr} (1 - \cos \theta_{\mathbf{K}, \mathbf{K}'}):$$

$$W_{\mathbf{K}, \mathbf{K}'}^{ex-sr} = \frac{2\pi}{\hbar} \langle |\langle \mathbf{K}' | V_{sr} | \mathbf{K} \rangle|^2 \rangle_{av.} \delta(E_{\mathbf{K}'} - E_{\mathbf{K}}), \quad (25)$$

where $\theta_{\mathbf{K}, \mathbf{K}'}$ is the angle between \mathbf{K} and \mathbf{K}' .

IV. NUMERICAL EVALUATION AND DISCUSSIONS

In this section, we evaluate the interlayer drag rate τ_{12}^{-1} in Eq. (10), the exciton scattering rate $\tau_{ex}^{-1} = \tau_{ex-ph}^{-1} + \tau_{ex-sr}^{-1}$, and the drag ratio \mathcal{R} between the drift velocities of the exciton and electron gases introduced in Eq. (12). We study how these quantities depend on the interlayer separation d , the temperature, the density of the electron gas, the hole mass m_h of the exciton, and the width of QW2 containing the exciton gas. The width of QW1 of the electron gas does not affect our result in the present approximation, as discussed earlier. However, the variational parameter λ introduced earlier for the exciton wave function depends on the QW2 width L_z and affects the interlayer interaction. Furthermore, L_z affects the exciton scattering rate due to phonons and interface roughness. The only condition assumed for the barrier in the present study is that it is wide and high enough to allow negligible penetration of the wave function. A possible enhancement of the exciton lifetime due to the drift motion is assessed.

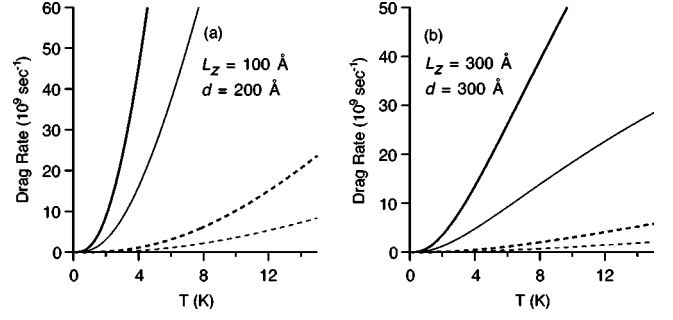


FIG. 2. The exciton drag rate τ_{12}^{-1} for two hole masses $m_h = 0.45$ (solid curves) and $m_h = 0.14$ (dashed curves) for two sets of parameters (a) $d = 200 \text{ \AA}$, $L_z = 100 \text{ \AA}$ and (b) $d = 300 \text{ \AA}$, $L_z = 300 \text{ \AA}$. Thick (thin) curves are for the electron density $N_{2D} = 1 \times 10^{11}$ ($N_{2D} = 2 \times 10^{11}$) cm^{-2} .

For the numerical study, we use $m^* = m_e = 0.067 m_o$ relevant for GaAs QWs, where m_o is the free electron mass. The hole mass is varied from $m_h = 0.14 m_o$ to $m_h = 0.45 m_o$, the former corresponding to a narrow well and the latter to a wide well. The above masses yield $a_B = 144.5 \text{ \AA}$ for $m_h = 0.14 m_o$ and $a_B = 112.5 \text{ \AA}$ for $m_h = 0.45 m_o$ for $\kappa = 12$. The RPA (random phase approximation) expression is employed for $\epsilon(q)$ (Ref. 13). Other parameters are $D_c = -6.5 \text{ eV}$, $D_v = 3.1 \text{ eV}$, $c_l = 5.14 \times 10^5 \text{ cm/s}$, $c_t = 3.04 \times 10^5 \text{ cm/s}$, $\rho = 5.3 \text{ g/cm}^3$, and $h_{14} = 1.2 \times 10^7 \text{ V/cm}$.¹¹ The variational parameter λ is taken from Ref. 9 and depends on the reduced width L_z/a_B of QW2. The interface-roughness parameters equal $\delta b = 5 \text{ \AA}$ and $\Lambda = 5 \text{ \AA}$.

The quantity τ_{ex-ph}^{-1} in Eq. (14) with $\eta_{\mathbf{K}, \mathbf{K}'} = 1$ is the lifetime scattering rate. In this expression, a full memory of the forward-going momentum is lost at each scattering event. As a result, it overestimates the exciton-phonon transport relaxation rate and thereby underestimates the field-induced exciton drift velocity in Eq. (12). The $\eta_{\mathbf{K}, \mathbf{K}'} = 1 - \cos \theta_{\mathbf{K}, \mathbf{K}'}$ factor in Eq. (25) accounts for the momentum loss in the forward direction. A similar exact relaxation-time solution for the transport equation is not possible for inelastic scattering in Eq. (14) at low temperatures. This momentum-loss factor arises from $1 - \cos \theta_{\mathbf{K}, \mathbf{K}'} = \mathbf{K} \cdot (\mathbf{K} - \mathbf{K}') / (\mathbf{K} \cdot \mathbf{K}) = 1 - \mathbf{K}' \cdot \mathbf{K} / K^2$ and takes a forward component out of the relative momentum loss through the collision. In order to make a correction for the momentum dissipation rate for exciton-phonon scattering beyond the $\eta_{\mathbf{K}, \mathbf{K}'} = 1$ approximation in Eq. (14), we try two models. In the first model we employ the same factor,

$$\eta_{\mathbf{K}, \mathbf{K}'} = 1 - \mathbf{K}' \cdot \mathbf{K} / K^2, \quad (26)$$

as in the elastic scattering case. For the second model, we replace the denominator of the second term of Eq. (26) by the average over the initial and final states, i.e., $K^2 \rightarrow (K^2 + K'^2)/2$, obtaining

$$\eta_{\mathbf{K}, \mathbf{K}'} = 1 - 2\mathbf{K}' \cdot \mathbf{K} / (K^2 + K'^2). \quad (27)$$

Figure 2 displays the temperature dependence of the drag rate τ_{12}^{-1} obtained from Eq. (10) for the two hole masses $m_h = 0.45 m_o$ (solid curves) and $m_h = 0.14 m_o$ (dashed curves) for two sets of parameters (a) $d = 200 \text{ \AA}$, $L_z = 100 \text{ \AA}$, and (b) d

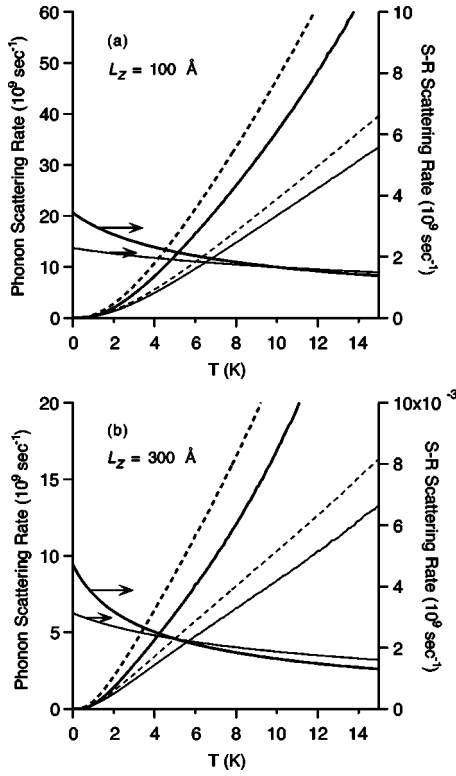


FIG. 3. Exciton scattering rate for two hole masses $m_h=0.45$ (thick curves) and $m_h=0.14$ (thin curves) for two different widths of the QW (a) $L_z=100$ Å and (b) $L_z=300$ Å. The two solid curves near the bottom of (a) and (b) indicate the scattering rate due to surface roughness (SR) (right axis). Other curves (left axis) indicate the momentum relaxation rate (solid curves) and the lifetime relaxation rate (dashed curves) due to electron-phonon scattering, respectively.

$=300$ Å, $L_z=300$ Å, for example, for 100-Å-wide QW1 and a 100-Å-wide barrier. As a result of an earlier approximation neglecting the QW1 width in Eq. (8) and taking the barrier infinitely high for the form factor in Eq. (15), the only restriction for the width of QW1 and the barrier width is that d equals the barrier width plus half the sum of the two QW widths. The thick and thin curves in Fig. 2 represent the electron density $N_{2D}=1 \times 10^{11}$ and $N_{2D}=2 \times 10^{11}$ cm $^{-2}$, respectively. Small momentum transfer processes dominate the interlayer drag because the excitons have small thermal energy and momentum at low temperatures. The drag rate decreases with increasing d and the electron density. It also decreases rapidly as m_h decreases toward the value of m_e mainly due to the cancellation between the electron-electron and electron-hole contributions in Eq. (8) in the limit $m_h = m_e$ (i.e., $\varphi_{e,q} = \varphi_{h,q}$).

The exciton scattering rate is displayed in Fig. 3 for two hole masses $m_h=0.45$ (thick curves) and $m_h=0.14$ (thin curves) for (a) $L_z=100$ Å and (b) $L_z=300$ Å. The two solid curves near the bottom of (a) and (b) are the scattering rate due to surface-roughness (right axis). Other solid and dashed curves indicate, respectively, the momentum relaxation rate and the lifetime relaxation rate (i.e., $\eta=1$) due to electron-phonon scattering (left axis). The two models in Eqs. (26) and (27) yield results indistinguishable from each other in Fig. 3(b) and very small differences in Fig. 3(a), where only

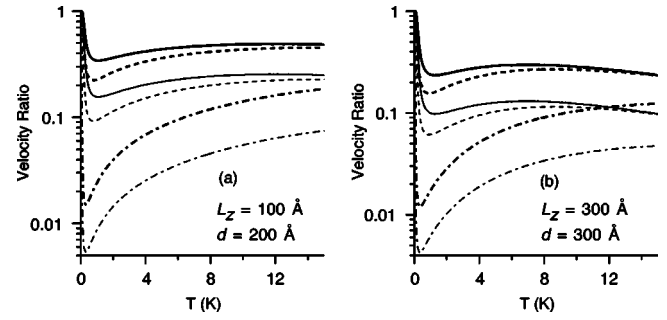


FIG. 4. Ratio of the drift velocities of the excitons and the electrons with only exciton-phonon scattering present for two sets of parameters (a) $d=200$ Å, $L_z=100$ Å and (b) $d=300$ Å, $L_z=300$ Å for $N_{2D}=1 \times 10^{11}$ cm $^{-2}$ (thick curves) and $N_{2D}=2 \times 10^{11}$ cm $^{-2}$ (thin curves). The hole mass equals $m_h=0.45m_0$ (solid curves), $m_h=0.35m_0$ (dashed curves), and $m_h=0.14m_0$ (dash-dotted curves).

the results from Eq. (27) are shown. The momentum relaxation rate is significantly smaller than the lifetime relaxation rate, as expected. The surface-roughness scattering rate decreases with increasing T because the exponential coherence factor in Eq. (24) decreases for a larger momentum transfer q_{\parallel} expected at higher temperatures. A large difference in the surface-roughness scattering rates between the two wells is due to the L_z^{-6} dependence in Eq. (24).

Figure 4 displays the intrinsic drag ratio, namely the ratio of the drift velocities of the excitons and the electrons, obtained from Eq. (12), with only exciton-phonon scattering without interface roughness for two sets of parameters (a) $d=200$ Å, $L_z=100$ Å and (b) $d=300$ Å, $L_z=300$ Å. The thick (thin) curves are for the density $N_{2D}=1 \times 10^{11}$ ($N_{2D}=2 \times 10^{11}$) cm $^{-2}$ for $m_h=0.45m_0$ (solid curve), $m_h=0.35m_0$ (dashed curve), and $m_h=0.14m_0$ (dash-dotted curve). The velocity ratio converges to unity for $T \rightarrow 0$ for all the curves owing to the fact that the exciton-phonon scattering rate τ_{ex-p}^{-1} drops faster than the interlayer drag rate τ_{12}^{-1} for $T \rightarrow 0$. These results indicate that the drift velocity of the excitons can be a significant fraction of that of the electrons.

Figure 5 shows the drag ratio with both exciton-phonon and interface-roughness scattering present for two sets of parameters: (a) $d=200$ Å, $L_z=100$ Å and (b) $d=300$ Å, $L_z=300$ Å. The thick (thin) curves are for the density $N_{2D}=1 \times 10^{11}$ ($N_{2D}=2 \times 10^{11}$) cm $^{-2}$ for $m_h=0.45m_0$ (solid curve), $m_h=0.35m_0$ (dashed curve), and $m_h=0.14m_0$ (dash-dotted curve). The velocity ratio decreases rapidly with decreasing T at low temperatures, unlike in Fig. 4, because the surface-roughness scattering rate saturates at low temperatures while the interlayer scattering rate τ_{12}^{-1} keeps decreasing with T . These results again indicate that the drift velocity of the excitons can be a good fraction of that of the electrons, except at very low temperatures.

Figure 6 shows (a) the drag rate τ_{12}^{-1} and (b) the ratio of the drift velocities at $T=4$ K as a function of d in the presence of exciton-phonon and exciton-surface-roughness scattering for $L_z=300$ Å and $N_{2D}=1 \times 10^{11}$ cm $^{-2}$ (thick curves) and $N_{2D}=2 \times 10^{11}$ cm $^{-2}$ (thin curves). The hole mass equals $m_h=0.45m_0$ (solid curves), $m_h=0.35m_0$ (dashed curves), and $m_h=0.14m_0$ (dash-dotted curves). Exciton-phonon scattering

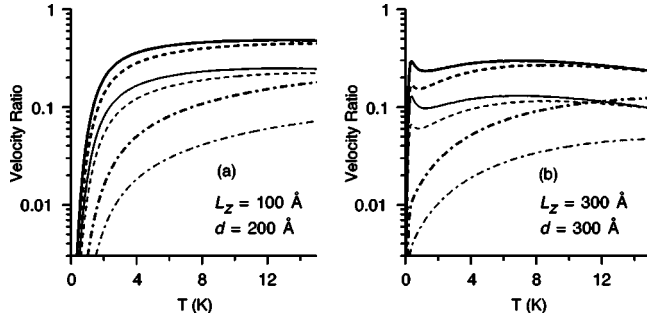


FIG. 5. Ratio of the drift velocities of the excitons and the electrons in the presence of exciton-phonon and exciton-surface-roughness scattering for two sets of parameters (a) $d=200$ Å, $L_z=100$ Å and (b) $d=300$ Å, $L_z=300$ Å for $N_{2D}=1 \times 10^{11}$ cm $^{-2}$ (thick curves) and $N_{2D}=2 \times 10^{11}$ cm $^{-2}$ (thin curves). The hole mass equals $m_h=0.45m_o$ (solid curves), $m_h=0.35m_o$ (dashed curves), and $m_h=0.14m_o$ (dash-dotted curves).

dominates surface-roughness scattering at this temperature and the effect of the latter is negligible. The drag rate and the velocity ratio follow poor exponential behavior and poor power-law behavior in the range of d shown.

It is shown in the above analysis that interlayer drag can induce a significant exciton drift velocity by fabricating a structure with optimal conditions. Some of these are (1) high electron mobility in the electron gas, (2) reduced friction for the excitons achieved by a wide well with smooth interfaces, and (3) large electron-hole asymmetry (i.e., $m_h \gg m_e$) for the exciton. A wide well is favorable for condition (3) for GaAs/ $\text{Al}_x\text{Ga}_{1-x}\text{As}$ QW. As seen from Fig. 5(a) and also from Eq. (12), a large elastic scattering rate of the excitons due to surface roughness (or impurities) can result in a very small drag ratio at low temperatures, where τ_{12}^{-1} is small. It is also desirable to have a thin barrier with a large barrier height to reduce d . The exciton can drift over a significant distance during its lifetime. The observed exciton lifetime in QWs varies widely depending on the sample condition and the QW width.^{14–17} Previous data indicate $\tau_R=2 \times 10^{-9}$ s for a 170 Å GaAs QW at 5 K, approaching the bulk value¹⁸ $\tau_R=3.3 \times 10^{-9}$ s for much wider wells.¹⁴ For $\mathcal{R}=0.2$, Δv_e

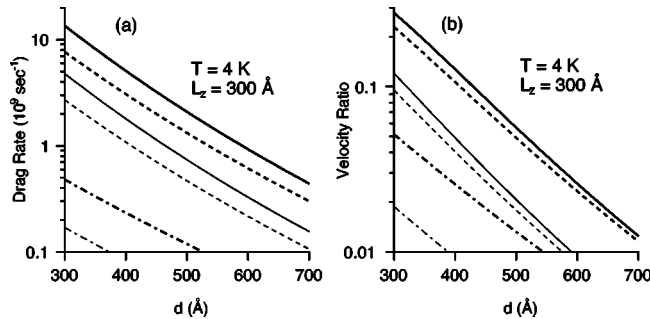


FIG. 6. (a) The drag rate τ_{12}^{-1} and (b) the ratio of the drift velocities of the excitons and the electrons as a function of the distance d in the presence of exciton-phonon and exciton-surface-roughness scattering for $L_z=300$ Å and $N_{2D}=1 \times 10^{11}$ cm $^{-2}$ (thick curves) and $N_{2D}=2 \times 10^{11}$ cm $^{-2}$ (thin curves). The hole mass equals $m_h=0.45m_o$ (solid curves), $m_h=0.35m_o$ (dashed curves), and $m_h=0.14m_o$ (dash-dotted curves).

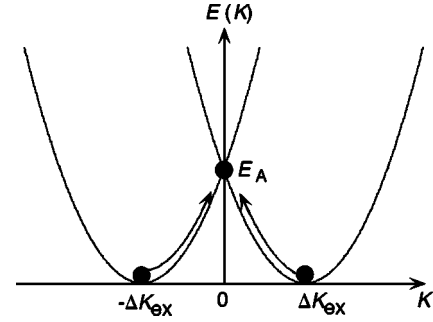


FIG. 7. A schematic diagram of the displaced energy-dispersion of excitons represented by black dots. The arrows indicate activation to $K=0$ point with an activation energy E_A for radiative decay.

$=10^6$ cm/s, and the lifetime $\tau_R=2 \times 10^{-9}$ s, the drift length equals $\mathcal{R}\Delta v_e\tau_R=4$ μm.

An exciton drifting with $\Delta K_{ex}=M\Delta\mathbf{V}_{ex}/\hbar$ cannot emit a photon until it is activated to the $K=0$ position, as illustrated in Fig. 7 by arrows. The activation energy is given in Kelvin by

$$E_A = \frac{1}{2}M\Delta v_{ex}^2 \approx 330(M/m_o)(\mathcal{R}\tilde{v}_e)^2 \text{ K}, \quad (28)$$

where \tilde{v}_e is the electron drift velocity in units of 10^7 cm 2 /Vs. The natural lifetime of the exciton will be enhanced by the factor $\tau_R \propto \exp(E_A/k_B T)$, which can be significant for optimal conditions. The radiative decay rate will have a Gaussian dependence $\tau_R^{-1} \propto \exp(-MR^2\mu^2 E^2/2k_B T)$ on E , where μ is the electron mobility. A similar displacement $\Delta K_{ex} \propto B$ of the exciton wave vector in K space is induced by an in-plane magnetic field B for indirect excitons, where the electron and the hole are spatially separated in the z direction perpendicular to the QW.^{19,20} In this case, a Gaussian dependence of $\tau_R^{-1} \propto \exp(-CB^2/k_B T)$ on B was observed¹⁹ as expected, where C is a constant.

V. CONCLUSIONS

An electric current in a high-mobility quasi-two-dimensional electron layer was shown to induce a significant drift of excitons in an adjacent layer through Coulomb interaction. The ratio between the drift velocities of the excitons and the electrons was calculated as a function of the temperature and the separation between the two gases at low temperatures. This ratio depends on the transport relaxation time of the exciton. The contribution to the latter from exciton-phonon and surface-roughness scattering was calculated. The estimated exciton drift velocity is a significant fraction of that of the electrons. The drift length was estimated to be of the order of micrometers or larger during the typical exciton lifetime for GaAs quantum wells. The exciton drift can be observed by a standard space- and time-resolved photoluminescence measurement. A possible enhancement of the exciton radiative lifetime due to drift was discussed.

The present model assumes that QW2 contains only stable charge-neutral incoherent excitons in equilibrium with the electron gas and the lattice in the absence of the applied

field. This situation prevails optimally under resonant excitation which creates coherent excitons that decay quickly into incoherent excitons through phonon scattering.²¹ We have also neglected the presence of stable free electrons or holes in QW2 which can be accelerated by the field, imparting momentum to the excitons. The momentum transfer through intra-QW collision will be more efficient than the interlayer transfer studied in this paper due to the physical proximity of the carriers and the excitons. The relative importance of this effect depends on the ratio of the electron density in QW1 and the density of the free carriers as well as the mobility of the free carriers and is not studied here. Excitons are also created through nonresonant excitation above the band gap into the unbound electron-hole continuum. In this case, the exciton formation time varies from tens to hundreds of picoseconds, depending on the carrier density.^{21,22} The role of excitons and electron-hole plasma in exciton luminescence as well as the question of whether the exciton lifetime can be shorter than the formation time is still under debate.^{22,23} Radiative decay times extracted from photoluminescence measurements should be taken with caution. For short exciton lifetimes \sim tens of picoseconds,^{14,15} the excitons may even be in nonequilibrium where the light cone is depleted, yielding a long exciton lifetime and resulting in a compromise between these too opposing effects. The estimated depletion rate²⁴ from the light cone through phonon scattering in GaAs QW, for example, is about $6 \times 10^{10} \text{ s}^{-1}$ at 5 K. If this situation prevails, the drag-induced enhancement of the exciton lifetime proposed in this paper will be less drastic.

The Born approximation employed for interlayer scattering in Eq. (1) is valid only when the damping through electron-exciton interaction is much smaller than the Fermi

energy ε_F of the electron gas as well as the average exciton energy in QW2. In order to demonstrate that this situation prevails in our system, we note that the factor q_{\parallel}^2 in the expression for τ_{12}^{-1} in Eq. (10) is roughly related to the thermal energy of the excitons via $(\hbar q_{\parallel})^2/2M \sim \eta \times k_B T$, where η is of the order of unity. The rest of the quantity in τ_{12}^{-1} is then proportional to the thermal average of the exciton damping $\langle \Gamma_{ex-e} \rangle$ due to interlayer scattering by electrons, resulting in $\langle \Gamma_{ex-e} \rangle \sim \hbar m^*/(2\eta M \tau_{12})$. It is clear from Fig. 2 that this quantity is much smaller than the typical exciton energy $k_B T$. Electron damping near the Fermi energy Γ_{F-ex} due to interlayer interaction with the exciton gas is found from Eq. (10) by replacing $f_{\mathbf{k}}^{(0)}=1$ and omitting the summation on \mathbf{k} . Noting that the \mathbf{k} summation in Eq. (10) yields $\sim k_B T \rho_F$ times the summand at the Fermi level, where ρ_F is the density of states, we estimate $\Gamma_{F-ex} \sim 1.2[\hbar m_o n_{ex}/(\eta M \tau_{12} k_B T)] \times 10^{-2} \text{ meV}$, where n_{ex} is the exciton density in units of 10^{10} cm^{-2} . It is clear from Fig. 2 that the quantity Γ_{F-ex} is much smaller than $\varepsilon_F=3.6 \text{ meV}$ (thick curves) and $\varepsilon_F=7.2 \text{ meV}$ (thin curves) for $n_{ex} \sim 1$ in the temperature regime shown.

ACKNOWLEDGMENTS

The author wishes to thank the faculty of the Department of Physics of KAIST for their hospitality, where part of this work was carried out. Sandia is a multiprogram laboratory operated by Sandia Corporation, a Lockheed Martin Company, for the U.S. DOE under Contract No. DE-AC04-94AL85000.

*Permanent address.

- ¹For Frenkel exciton transport, see T. Holstein, S. K. Lyo, and R. Orbach, p. 39, in *Laser Spectroscopy of Solids*, edited by W. M. Yen and P. M. Selzer, *Topics in Applied Physics*, 2nd ed. (Springer-Verlag, New York, 1986), Vol. 49.
- ²For Wannier exciton transport, see T. Takagahara, *Phys. Rev. B* **31**, 6552 (1985) and Ref. 3.
- ³S. K. Lyo, *Phys. Rev. B* **62**, 13 641 (2000).
- ⁴C. Rocke, S. Zimmermann, A. Wixforth, J. P. Kotthaus, G. Böhm, and G. Weimann, *Phys. Rev. Lett.* **78**, 4099 (1997).
- ⁵M. M. de Lima, Jr., R. Hey, J. A. H. Stotz, and P. V. Santos, *Appl. Phys. Lett.* **84**, 2569 (2004).
- ⁶L. Zheng and A. H. Mac Donald, *Phys. Rev. B* **48**, 8203 (1993).
- ⁷For a review, see A. G. Rojo, *J. Phys.: Condens. Matter* **11**, R31 (1999), and references therein.
- ⁸J. M. Ziman, *Principles of the Theory of Solids*, 2nd ed. (Cambridge University Press, Cambridge, 1995), p. 211.
- ⁹Y. Shinozuka and M. Matsuura, *Phys. Rev. B* **28**, 4878 (1983).
- ¹⁰T. Holstein, *Ann. Phys. (N.Y.)* **29**, 410 (1964).
- ¹¹S. K. Lyo, *Phys. Rev. B* **40**, 6458 (1989).
- ¹²S. K. Lyo, *J. Phys.: Condens. Matter* **13**, 1259 (2001).
- ¹³F. Stern, *Phys. Rev. Lett.* **18**, 546 (1967).
- ¹⁴J. Feldmann, G. Peter, E. O. Göbel, P. Dawson, K. Moore, C.

- Foxon, and R. J. Elliott, *Phys. Rev. Lett.* **59**, 2337 (1987).
- ¹⁵B. Deveaud, F. Cle'rot, N. Roy, K. Satzke, B. Sermage, and D. S. Katzer, *Phys. Rev. Lett.* **67**, 2355 (1991).
- ¹⁶M. Gurioli, A. Vinattieri, M. Colocci, C. Deparis, J. Massies, G. Neu, A. Bosacchi, and S. Franchi, *Phys. Rev. B* **44**, 3115 (1991).
- ¹⁷J. Martinez-Pastor, A. Vinattieri, L. Carraresi, M. Colocci, Ph. Roussignol, and G. Weimann, *Phys. Rev. B* **47**, 10 456 (1993).
- ¹⁸G. W. 't Hooft, W. A. J. A. van der Poel, L. W. Molenkamp, and C. T. Foxen, *Phys. Rev. B* **35**, 8281 (1987).
- ¹⁹A. Parangeli, P. C. M. Christianen, J. C. Mann, I. V. Tokatly, C. B. Soerensen, and P. E. Lindelof, *Phys. Rev. B* **62**, 15 323 (2000).
- ²⁰S. K. Lyo, *Phys. Rev. B* **64**, 201317 (2001).
- ²¹R. A. Kaindl, M. A. Carnahan, D. Hägelle, R. Lövenich, and D. S. Chemla, *Nature (London)* **423**, 734 (2003).
- ²²J. Szczytko, L. Kappei, J. Berney, F. Morier-Genoud, M. T. Portella-Oberli, and B. Deveaud, *Phys. Rev. Lett.* **93**, 137401 (2004).
- ²³S. Chatterjee, C. Ell, S. Mosor, G. Khitrova, H. M. Gibbs, W. Hoye, M. Kira, S. W. Koch, J. P. Prineas, and H. Stolz, *Phys. Rev. Lett.* **92**, 067402 (2004).
- ²⁴E. Hanamura, *Phys. Rev. B* **38**, 1228 (1988).